



HAL
open science

Analysis and Control of Multi-timescale Modular Directed Heterogeneous Networks

Anes Lazri, Elena Panteley, Antonio Loria

► **To cite this version:**

Anes Lazri, Elena Panteley, Antonio Loria. Analysis and Control of Multi-timescale Modular Directed Heterogeneous Networks. 2023. hal-04266142

HAL Id: hal-04266142

<https://hal.science/hal-04266142>

Preprint submitted on 31 Oct 2023

HAL is a multi-disciplinary open access archive for the deposit and dissemination of scientific research documents, whether they are published or not. The documents may come from teaching and research institutions in France or abroad, or from public or private research centers.

L'archive ouverte pluridisciplinaire **HAL**, est destinée au dépôt et à la diffusion de documents scientifiques de niveau recherche, publiés ou non, émanant des établissements d'enseignement et de recherche français ou étrangers, des laboratoires publics ou privés.

Analysis and Control of Multi-timescale Modular Directed Heterogeneous Networks

Anes Lazri Elena Panteley Antonio Loría

Abstract— We examine the collective behavior of large-scale networks of heterogeneous nonlinear systems with directed weighted interconnections, and containing a spanning tree. We consider networks that are composed of groups of densely interconnected nodes, called modules, that are in turn sparsely interconnected. Such networks are called modular. The modules represent sub-networks wherein consensus may be rapidly achieved, while synchronization among modules occurs at a lower pace. Furthermore, relying on the framework of [1], we identify an underlying dynamics that corresponds to a weighted average of the nodes' respective states. This average dynamics evolves on a yet slower time-scale. Such triple time-scale make modular networks are amenable to be analyzed via singular-perturbations theory. We show that if the nodes' dynamics are semi-passive and the average dynamics is globally asymptotically stable, so is the entire network. In the case that the average dynamics is not globally asymptotically stable we show how our main analysis statement can be used for network control, via the addition of control nodes, in order to globally asymptotically stabilize the network.

I. INTRODUCTION

Modular networks consist in sub-networks, called modules, of densely interconnected nodes, while the interconnections amongst these modules are comparatively weaker [2]–[4]. The notion of grouping multiple agents in a single module has been employed extensively in diverse contexts, whether for undirected networks [5], [6], [7], or for directed networks [8], [9]. Empirical observations have consistently revealed that, subject to certain topological conditions, agents within the same module tend to converge toward local consensus among themselves rapidly. However, achieving global consensus among modules transpires at a relatively slower pace when compared to intra-modular convergence. When the interconnection within modules is sufficiently high, obtaining a reduced model representing the overall emerging dynamics becomes feasible [7], [10].

In [11] singular-perturbations theory is used to model a heterogeneous network with high coupling gain. As it is explained therein, the network dynamics can be separated into a slow system representing the emergent behavior of the network and a fast one representing synchronization errors. This two-time scale modeling approach provides insights into the emergent behavior of the network. Similarly, in [12], singular-perturbation techniques are applied to study interconnected

linear systems with switching interconnection topology and linear coupling. It is showed therein that when the coupling gain is sufficiently high, the synchronized behavior of the network can be approximated by a reduced-order switching system. This reduction in complexity allows for a simplified analysis of the network dynamics.

The idea of using time scale separation for sparse dynamic networks probably originates from [13], where a two-time scale model is developed to approximate the behavior of a modular network or sparsely connected modules of densely connected agents, specifically focusing on the consensus problem for linear systems. This concept is further expanded in [5], which investigates nonlinear networks with internally dense and externally sparse interconnections. The study emphasizes the synchronization of densely connected nodes within certain areas, which dominate the slow dynamics of the network.

In [14], for undirected networks of linear systems, the authors explore modular networks with linear dynamics and emphasize the presence of three-time scales in the synchronization of interconnected agents in modular networks. Then, under some assumptions, the network dynamics can be approximated using a two-parameter singular-perturbation form. The mean-field dynamics evolve on the slowest time scale, intra-modular dynamics on the fastest, and inter-modular dynamics are faster than mean-field but slower than intra-modular dynamics. These insights enhance the understanding of multi-scale synchronization in modular networks.

In this paper we analyze modular networks using a triple-time-scale model and give mild sufficient conditions for global asymptotic stability of the origin. Relative to [14] we consider directed networks of heterogeneous nonlinear semi-passive [15] systems. Relative to [11] we consider networks evolving in three time scales. Moreover, we provide a control method to stabilize the network. The method is conceptually reminiscent of pinning control, which is a technique that involves controlling a subset of nodes to synchronize the entire network [16]. However, such a strategy does not consider the multiple time-scale behavior of modular networks.

In Section II we present our standing hypotheses and give a preliminary statement on boundedness of solutions for generic directed networks; in Section III we describe the three-time-scale model. Section IV we present our main statement on stability analysis; in Section V we describe our control method and provide illustrative examples. The paper is wrapped up with some concluding remarks, given in Section VI.

A. Lazri is with L2S, CNRS, Univ Paris-Saclay, France (e-mail: anes.lazri@centralesupelec.fr) E. Panteley and A. Loría are with L2S, CNRS, (e-mail: {elena.panteley,antonio.loria}@cnrs.fr).

II. MODEL AND PROBLEM FORMULATION

Let us consider N nonlinear dynamical systems

$$\dot{\chi}_i = f_i(\chi_i) + \nu_i, \quad i \leq N, \quad \chi_i \in \mathbb{R}^n, \quad (1)$$

where the functions f_i are continuously differentiable and ν_i are inputs defined as

$$\nu_i := - \sum_{j=1}^N \sigma_{ij} a_{ij} (\chi_i - \chi_j), \quad (2)$$

where a_{ij} represents the (in)existence of a link between two agents and σ_{ij} represents the coupling strength. More precisely, $a_{ij} > 0$ and $\sigma_{ij} > 0$ if there is an interconnection arc from the j th node to the i th one and $a_{ij} = \sigma_{ij} = 0$ otherwise. In the case that all the interconnection strengths σ_{ij} are equal, say $\sigma_{ij} =: \sigma$, the networked system, in compact form, reads

$$\dot{\chi} = \mathcal{F}(\chi) - \sigma \mathcal{L}\chi, \quad (3)$$

where χ and \mathcal{F} are vectors whose elements are χ_i and f_i , \mathcal{L} is a Laplacian matrix, whose elements are defined as

$$\ell_{i,j} = \begin{cases} -a_{ij}, & i \neq j \\ \sum_{\substack{\ell=1 \\ \ell \neq i}}^N a_{i\ell}, & i = j, \quad i, j \leq N. \end{cases}$$

In this paper we consider the case in which certain links have an interconnection strength $\sigma_{ij} := \sigma^I$ and for others $\sigma_{ij} := \sigma^E$, where $\sigma^I \gg \sigma^E \geq \sigma^*$, where $\sigma^* > 0$ is a certain threshold. In addition, it is assumed that there are many more arcs with strength σ^I than with strength σ^E . By virtue of this, the networked systems are naturally organized into densely interconnected modules that are sparsely interconnected among themselves. A well-known example of such network, which we refer to as *modular*, is that of power distribution [13].

We are primarily interested in investigating sufficient conditions to guarantee global asymptotic stability of the origin for modular networks, but also in devising control design strategies to stabilize the origin. To those ends, we start by introducing a more suitable model that consists in a (non-unique) modular network decomposition. Such model is defined by relabeling the network's nodes and the systems' states and introducing an adequate notation.

We consider that under the assumptions made above on the coupling strength, m modules are formed, labeled M_k with $k \leq m$, and each containing N_k systems densely connected with high coupling strength. That is, each of such modules forms a sub-network of N_k nonlinear systems, whose models (1) are rewritten using a notation that makes explicit the module-dependency, *i.e.*,

$$\dot{x}_{k,i} = f_{k,i}(x_{k,i}) + u_{k,i}, \quad k \leq m, \quad i \leq N_k, \quad (4)$$

where $x_{k,i} \in \mathbb{R}^n$ denotes the state of the i th system within the k th module, and $f_{k,i}$ and $u_{k,i}$ define its dynamics and input respectively. Then, to distinguish the interconnection links depending on the coupling strength, the inputs are split in two parts as follows:

$$u_{k,i} = u_{k,i}^I + u_{k,i}^E, \quad (5a)$$

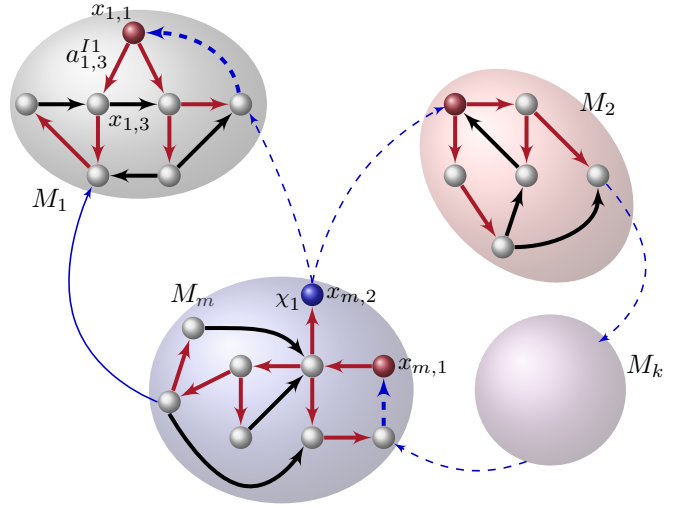


Fig. 1. Schematic representation of a directed modular network composed of m modules M_k , each constituting a sub-network. Within each module the interconnections are “strong” and dense (represented by thick arrows) while among modules the interconnections are of lesser strength and more sparse (represented by thinner arrows). Each module contains a directed spanning tree—represented by red arrows within the modules and with a root node also in red. The overall network also contains a directed spanning tree—represented by dashed blue and solid red arrows and with an overall root node represented in blue. This node is first in the overall network so it is originally labeled χ_1 —see Eq. 1, but it does not necessarily correspond to the root of a module’s spanning tree. Indeed, it corresponds to the 2nd node in the m th module, so its state is $x_{m,1}$ in Eq. (4).

$$u_{k,i}^I = -\sigma^I \sum_{j=1}^{N_k} a_{ij}^{I,k} (x_{k,i} - x_{k,j}), \quad (5b)$$

$$u_{k,i}^E = -\sigma^E \sum_{\substack{\ell \neq k \\ \ell=1}}^m \sum_{j=1}^{N_\ell} a_{ij}^{E,k} (x_{k,i} - x_{\ell,j}). \quad (5c)$$

In the previous expressions, $a_{ij}^{I,k}$ and $a_{ij}^{E,k}$ are zero- or positive-valued, depending on the existence or absence of a link between two nodes within one module or between two modules respectively—see Figure 1 for an illustration.

Then, in compact form, we define the vectors of rearranged nodes’ states and dynamics,

$$x := \begin{bmatrix} x_{1,1} \\ \vdots \\ x_{1,N_1} \\ \vdots \\ x_{m,1} \\ \vdots \\ x_{m,N_m} \end{bmatrix} \in \mathbb{R}^{Nn}, \quad F(x) := \begin{bmatrix} f_{1,1}(x_{1,1}) \\ \vdots \\ f_{1,N_1}(x_{1,N_1}) \\ \vdots \\ f_{m,1}(x_{m,1}) \\ \vdots \\ f_{m,N_m}(x_{m,N_m}) \end{bmatrix} \quad (6)$$

which contain all the states χ_i and respective dynamics f_i in (1), but not necessarily in the original order $[\chi_1^\top \cdots \chi_N^\top]^\top$. Note that $x = T\chi$ where T is a permutation matrix (hence invertible). With this notation, the closed-loop networked system (4)–(5), takes the form,

$$\dot{x} = F(x) - \sigma^I [L^I \otimes I_n]x - \sigma^E [L^E \otimes I_n]x \quad (7)$$

where $v := [[v_{1,1}^\top \cdots v_{1,N_1}^\top] \cdots [v_{m,1}^\top \cdots v_{m,N_m}^\top]]^\top$, and L^I

and L^E are Laplacian matrices defined as follows.

$$L^I := \text{blockdiag}[L_1^I \ L_2^I \ \cdots \ L_m^I], \quad (8a)$$

$$L_k^I := [\ell_{i,j}^{Ik}] \quad (8b)$$

$$\ell_{i,j}^{Ik} := \begin{cases} -a_{ij}^{Ik}, & i \neq j \\ \sum_{\substack{\ell=1 \\ \ell \neq i}}^{N_k} a_{i\ell}^{Ik}, & i = j, \end{cases} \quad (8c)$$

where, for each fixed $k \leq m$, $a_{ij}^{Ik} > 0$ if there is an interconnection arc from the j th node to the i th one within the k th module and $a_{ij}^{Ik} = 0$ otherwise; $L^E \in \mathbb{R}^{N \times N}$, which corresponds to the intra-modular Laplacian, is defined as $L^E = L - L^I$, where $L = T\mathcal{L}T^{-1}$. Both matrices L^I and L^E are Laplacians. Moreover, under the following assumption, L_k^I contains exactly one eigenvalue with null real part.

Assumption 1 (topology): Each module M_k individually forms a strongly-connected sub-network; its topology is captured by the Laplacian L_k^I with elements defined in (8c). Furthermore, both, the overall network and the network of modules, contain a spanning tree. In addition, the interconnection strengths satisfy $\sigma^E|L^E| < \sigma^I|L^I|$, where $|\cdot|$ denotes the induced L_2 norm. \square

Remark 1: There is little loss of generality in assuming that each module M_k is strongly connected because in the primary setting the modules are densely connected. The last part of Assumption 1 means that, for each agent, the intra-modular influence is higher than the inter-modular influence. In other words, either the interconnections within modules are denser than the interconnections among them or the interaction weights inside modules is higher than among them.

The rest of the paper is devoted to the stability analysis of, and control design for, Equation (7) under Assumption 1. To that end, we also pose the following hypothesis on the individual systems' dynamics.

Assumption 2 (regularity and passivity): For each pair (k, i) , the function $f_{k,i}$ in (4) is continuously differentiable and admits the origin as a unique equilibrium. In addition, all the units (1) are semi-passive [15] with respect to the input $u_{k,i}$ and the output $x_{k,i}$, with continuously differentiable and radially unbounded storage functions $V_{k,i} : \mathbb{R} \rightarrow \mathbb{R}_{\geq 0}$. That is, there exist positive definite and radially unbounded storage functions $V_{k,i}$, positive constants $\rho_{k,i}$, continuous functions $H_{k,i}$, and non-negative continuous functions $\psi_{k,i}$ such that

$$\dot{V}_{k,i}(x_{k,i}) \leq x_{k,i}u_{k,i} - H_{k,i}(x_{k,i})$$

and $H_{k,i}(x_{k,i}) \geq \psi_{k,i}(|x_{k,i}|)$ for all $|x_{k,i}| \geq \rho_{k,i}$. \square

The hypothesis of semi-passivity, which is little restrictive since it is satisfied by a number of physical systems, is useful to establish that the solutions of the networked system are bounded. The following self-contained statement generalizes [1, Proposition 2] by establishing boundedness of the network's trajectories, for arbitrary directed networks of heterogeneous semi-passive systems, containing a spanning tree. The proof is provided in [17].

Lemma 1: Consider a network of N interconnected dynamical systems as in (1)-(2), with f_i continuously differentiable,

admitting the origin as the unique equilibrium, and such that each map $\nu_i \mapsto \chi_i$ is semi-passive. Assume, in addition, that the network's graph contains a directed spanning tree. Then, the trajectories $t \mapsto \chi_i(t)$, for all $i \leq N$, solutions to (1)-(2), are globally bounded. \square

The statement of Lemma 1 follows from the observation that by reordering the network's states, in similar fashion as done in [18] for weakly connected graphs, the Laplacian matrix L may be transformed into that of a connected network that consists in a spanning-tree of strongly-connected sub-graphs, so the transformed Laplacian matrix possesses a convenient lower-block-triangular form (see [17, Lemma 2]). Then, the statement follows using a cascades argument, from the fact that the trajectories of each strongly-connected sub-graph are bounded (see the proof of [1, Proposition 2]) and remain bounded under the effect of the interconnections (see [17, Lemma 3]).

Assumptions 1 and 2 are also instrumental to cast the analysis of (7) within the framework established in [1], which builds on the recognition that the networked systems' collective behavior is dichotomous. It consists in two distinct dynamical components that evolve in orthogonal spaces, that of an emerging average system with state χ_s and that of the synchronization errors e_i , defined as the difference between the dynamics of each individual system and the average dynamics, i.e., $e_i := \chi_i - \chi_s$. More precisely, χ_s is a weighted average of χ_i s, defined via the left-eigenvector corresponding to the unique null eigenvalue of \mathcal{L} . In particular, if the synchronization manifold $\{i \leq N : e_i = 0\}$ is asymptotically stable the origin for the network system (7) is asymptotically stable if and only if so is $\{\chi_s = 0\}$.

In [19] it is recognized that global asymptotic stability of the origin for (3) is possible for sufficiently large values of σ . The analysis in this reference is based on the fact that the average dynamics $\dot{x}_s = f_s(x_s)$ evolves in scaled time t/σ , that is, much slower than the synchronization dynamics. For modular networks (7) the analysis starts with recognizing that the presence of two different coupling strengths entails *two* average dynamical systems, in addition to the synchronization dynamics of the individual systems. Each of these three dynamics evolves in a different time-scale. The fastest time-scale corresponds to that in which the synchronization errors within modules evolve; we call this the intra-modular dynamics. The second time-scale, which is moderately fast, corresponds to that of the synchronization errors amongst the modules. Then, a third and slowest time scale, corresponds to that in which evolves the average of the modules' averages. The dynamics evolving in the second and third time-scales constitute what we call inter-modular dynamics. The precise modeling of these three dynamical systems is the subject of the next section.

III. THREE-TIME-SCALES MODELING

Consider the system (7) under Assumptions 1 and 2.

A. Intra-modular dynamics

Let k be arbitrarily fixed and let us focus our attention on the k th module. It consists in a connected (sub)network

with Laplacian L_k^I , N_k nodes, and contains a spanning tree (Assumption 1). Therefore, L_k^I has a unique zero eigenvalue and $N_k - 1$ others with positive real part. The null eigenvalue has as an associated left eigenvector $v_{\ell k} := \frac{1}{N_k} \mathbf{1}_{N_k}$, with $\mathbf{1}_{N_k} := [1 \ 1 \cdots 1]^\top$ and the other $N_k - 1$ eigenvalues admit associated linearly independent eigenvectors that are gathered in the matrix $Q_k \in \mathbb{R}^{N_k \times (N_k - 1)}$. Therefore, L_k^I admits the Jordan decomposition

$$L_k^I = V_k \begin{bmatrix} 0 & 0 \\ 0 & \Lambda_k^I \end{bmatrix} V_k^{-1} \quad (9)$$

where $\Lambda_k^I \in \mathbb{R}^{(N_k - 1) \times (N_k - 1)}$ is positive definite and $V_k \in \mathbb{R}^{N_k \times N_k}$ is the invertible transformation matrix $V_k := [\mathbf{1}_{N_k} \ Q_k]$. Therefore,

$$V_k^{-1} =: \begin{bmatrix} v_{\ell k}^\top \\ Q_k^\dagger \end{bmatrix}. \quad (10)$$

Then, akin to [19], we introduce a set of new state variables, $\zeta_k \in \mathbb{R}^n$ and $\xi_k \in \mathbb{R}^{n_{N_k - 1}}$, defined as

$$\begin{bmatrix} \zeta_k \\ \xi_k \end{bmatrix} := \begin{bmatrix} [v_{\ell k}^\top \otimes I_n] \\ [Q_k^\dagger \otimes I_n] \end{bmatrix} \bar{x}_k,$$

where $\bar{x}_k := [x_{k,1}^\top \ x_{k,2}^\top \ \cdots \ x_{k,N_k}^\top]^\top$.

The state variable ζ_k may be regarded as the weighted average of the k th module's nodes' states while, ξ_k is a projection of the synchronization errors, e_k , relative to that average. More precisely, we define $e_k \in \mathbb{R}^{n_{N_k}}$ as

$$e_k := \bar{x}_k - [\mathbf{1}_{N_k} \otimes I_n] \zeta_k \quad (11)$$

$$= [Q_k \otimes I_n] \xi_k. \quad (12)$$

Note that all the systems within the module synchronize (that is, $x_{k,i} \rightarrow x_{k,j}$) if and only if $e_k \rightarrow 0$ or, equivalently, if and only if $\xi_k \rightarrow 0$. If, in addition, for the average system $\dot{\zeta}_k = [v_{\ell k}^\top \otimes I_n] \bar{x}_k$ we have $\zeta_k \rightarrow 0$, we conclude that $x_{k,i} \rightarrow 0$. The same reasoning applies to the stronger property of global asymptotic stability. Therefore, for our problem of interest, it is crucial to study the dynamic evolution of ζ_k and ξ_k . To that end, we gather these variables into the vectors $\zeta \in \mathbb{R}^{nm}$ and $\xi \in \mathbb{R}^{n_{N_k - 1} m}$, defined as $\zeta := [\zeta_1 \ \cdots \ \zeta_m]$ and $\xi := [\xi_1^\top \ \cdots \ \xi_m^\top]^\top$. The latter satisfy

$$\begin{bmatrix} \dot{\zeta} \\ \dot{\xi} \end{bmatrix} =: \begin{bmatrix} P^\dagger \otimes I_n \\ Q^\dagger \otimes I_n \end{bmatrix} x, \quad (13)$$

where x is defined in (6), $P \in \mathbb{R}^{N \times m}$ is defined as

$$P = \text{blockdiag}_{k \leq m} \{ \mathbf{1}_{N_k} \} \quad (14)$$

—cf. [20], $Q = \text{blockdiag}_{k \leq m} \{ Q_k \}$, $P = \text{blockdiag}_{k \leq m} \{ v_{\ell k} \}$ and $Q = \text{blockdiag}_{k \leq m} \{ Q_k^\dagger \}$. Note that, since $\mathbf{1}_{N_k}$ and the columns of Q_k form the orthogonal transformation V_k in (9), we have $\mathbf{1}_{N_k}^\top Q_k = 0$, so $P^\dagger Q = Q^\dagger P = 0$. In turn, after (13) it follows that

$$x = \bar{P} \zeta + \bar{Q} \xi, \quad (15)$$

where we defined $\bar{P} := [P \otimes I_n]$ and $\bar{Q} := [Q \otimes I_n]$. Now, differentiating on both sides of (13) and using (7) and (15), we obtain

$$\dot{\zeta} = \bar{P}^\dagger F(\bar{P} \zeta + \bar{Q} \xi) - \sigma^I \bar{P}^\dagger \bar{L}^I [\bar{P} \zeta + \bar{Q} \xi]$$

$$- \sigma^E \bar{P}^\dagger \bar{L}^E [\bar{P} \zeta + \bar{Q} \xi], \quad (16)$$

$$\dot{\xi} = \bar{Q}^\dagger F(\bar{P} \zeta + \bar{Q} \xi) - \sigma^I \bar{Q}^\dagger \bar{L}^I [\bar{P} \zeta + \bar{Q} \xi]$$

$$- \sigma^E \bar{Q}^\dagger \bar{L}^E [\bar{P} \zeta + \bar{Q} \xi], \quad (17)$$

where $\bar{L}^I := [L^I \otimes I_n]$, and $\bar{L}^E := [L^E \otimes I_n]$. However, note that $L_k^I \mathbf{1}_{N_k} = 0$, so $L^I P = P^\dagger L^I = 0$, while $\bar{Q}^\dagger \bar{L}^I \bar{Q} \xi = \bar{\Lambda}^I \xi$. Thus, (16) and (17) become

$$\dot{\zeta} = F_\zeta(\zeta, \xi) \quad (18a)$$

$$\dot{\xi} = -\sigma^I \bar{\Lambda}^I \xi + F_\xi(\zeta, \xi), \quad (18b)$$

where $\bar{\Lambda}^I := [\Lambda^I \otimes I_n]$ and $\Lambda^I \in \mathbb{R}^{(N-m) \times (N-m)}$ is defined as $\Lambda^I := \text{blockdiag}_{k \leq m} \{ \Lambda_k^I \}$, and

$$F_\zeta(\zeta, \xi) = \bar{P}^\dagger F(\bar{P} \zeta + \bar{Q} \xi) - \sigma^E \bar{P}^\dagger \bar{L}^E [\bar{P} \zeta + \bar{Q} \xi], \quad (19)$$

$$F_\xi(\zeta, \xi) = \bar{Q}^\dagger F(\bar{P} \zeta + \bar{Q} \xi) - \sigma^E \bar{Q}^\dagger \bar{L}^E [\bar{P} \zeta + \bar{Q} \xi]. \quad (20)$$

Equation (18a) corresponds to the dynamics of a network of modules, *i.e.*, a network of sub-networks. On the synchronization manifold $\{\xi = 0\}$ each module may be assimilated to a single node with dynamics $\dot{\zeta}_k = F_{\zeta_k}(\zeta, 0)$, but note that the dynamics of each module depends on that of other modules as well, so Eq. (18a) constitutes a reduced network of m nodes—cf. [21], [22], [23]. This is the inter-modular dynamics, which we study in detail next.

B. Inter-modular dynamics

To assess the behavior of the reduced network (18a) we start by applying on ζ a coordinate transformation similar to that defined above and performed on x . To that end, we observe that under Assumption 1 the network (18a) is also connected and contains a directed spanning tree. Furthermore, its associated Laplacian, which appears in the definition of $F_\zeta(\zeta, \xi)$ above, is given by

$$\tilde{L}^E := \begin{bmatrix} \bar{a}_{11}^E & -\bar{a}_{12}^E & \cdots & -\bar{a}_{1m}^E \\ \vdots & \ddots & & \vdots \\ \vdots & & \ddots & \vdots \\ -\bar{a}_{m1}^E & -\bar{a}_{m2}^E & \cdots & \bar{a}_{mm}^E \end{bmatrix}, \quad (21)$$

where, for any two modules indexed i and j , $\bar{a}_{ij}^E := v_{\ell i}^\top A_{ij} \mathbf{1}_{n_j}$ and A_{ij} is the $N_i \times N_j$ block of L^E gathering the edges from the i th to the j th module.

Thus, since there exists a directed spanning tree in the modules' interconnection graph, \tilde{L}^E admits the Jordan decomposition

$$\tilde{L}^E = W \begin{bmatrix} 0 & 0 \\ 0 & \Lambda^E \end{bmatrix} W^{-1}, \quad (22)$$

where $W \in \mathbb{R}^{m \times m}$ is nonsingular, and $\Lambda^E \in \mathbb{R}^{(m-1) \times (m-1)}$ is the diagonal matrix defined by the eigenvalues of \tilde{L}^E with positive real part, that is, $\Lambda^E := \text{diag}_{i \in \{2,3,\dots,m\}} \{ \lambda_i(\tilde{L}^E) \}$. As a matter of fact,

$$W = [\mathbf{1}_m \ W_1], \quad (23)$$

where W_1 is full-column-rank, so it is left-invertible and W has full rank. Therefore,

$$W^{-1} =: \begin{bmatrix} w_\ell^\top \\ W_1^\dagger \end{bmatrix}. \quad (24)$$

Next, we introduce the new state variables

$$\begin{bmatrix} x_e \\ \eta \end{bmatrix} = \begin{bmatrix} w_\ell^\top \otimes I_n \\ W_1^\dagger \otimes I_n \end{bmatrix} \zeta, \quad (25)$$

where $x_e \in \mathbb{R}^n$ corresponds to the ‘‘weighted average of averages ζ_k ’’, while η is a projection of all the synchronization errors among modules, $\zeta_k - x_e$. That is, the vector of synchronization errors corresponds to

$$e_\eta := \zeta - [\mathbf{1}_m \otimes I_n] x_e \quad (26a)$$

$$= [W_1 \otimes I_n] \eta. \quad (26b)$$

All the states of the reduced network (of modules) reach consensus with the x_e -system if and only if $\eta = 0$. Thus, the collective behavior of the reduced-network (18a) may be fully assessed by studying the equivalent dynamical system that results from differentiating on both sides of (25). That is,

$$\dot{x}_e = f_e(x_e, \eta, \xi) \quad (27a)$$

$$\dot{\eta} = -\sigma^E \bar{\Lambda}^E \eta + f_\eta(x_e, \eta, \xi), \quad (27b)$$

where

$$f_e(x_e, \eta, \xi) = [w_\ell^\top \otimes I_n] F_\zeta(\zeta, \xi), \quad (28)$$

$$f_\eta(x_e, \eta, \xi) = \bar{W}_1^\dagger \bar{P}^\dagger F_\zeta(\bar{P}\zeta + \bar{Q}\xi) - \sigma^E \bar{W}_1^\dagger \bar{P}^\dagger \bar{L}^E \bar{Q}\xi \quad (29)$$

$$\zeta = [\mathbf{1}_m \otimes I_n] x_e + [W_1 \otimes I_n] \eta, \quad (30)$$

and $\bar{\Lambda}^E := [\Lambda^E \otimes I_n]$. Equation (27a) follows by direct differentiation of $x_e = [w_\ell^\top \otimes I_n] \zeta$, using (25) and (18a). The expression (30) follows from (26). Equation (27b), together with (29), is obtained as follows. After (25), (18a), and (19), we have

$$\dot{\eta} = \bar{W}_1^\dagger \bar{P}^\dagger F(\bar{P}\zeta + \bar{Q}\xi) - \sigma^E \bar{W}_1^\dagger [\bar{P}^\dagger \bar{L}^E \bar{P}\zeta + \bar{P}^\dagger \bar{L}^E \bar{Q}\xi].$$

Now, by definition—see (21)— $\bar{P}^\dagger \bar{L}^E \bar{P} = [\tilde{L}^E \otimes I_n]$. Then, after (30) and the fact that $\tilde{L}^E \mathbf{1}_m = 0$, we have $\bar{W}_1^\dagger \bar{P}^\dagger \bar{L}^E \bar{P}\zeta = \bar{W}_1^\dagger [\tilde{L}^E \otimes I_n] \bar{W}_1 \eta$. Then, after (22) and (23), we obtain $\bar{W}_1^\dagger [\tilde{L}^E \otimes I_n] \bar{W}_1 = \bar{\Lambda}^E$.

C. Multi-timescale overall network dynamics

After the previous developments, we see that the network model (7) is equivalent to Eqs. (27) and (18b). Now we define the singular parameter $\varepsilon_E := 1/\sigma^E$ and the ratio of influence among and within modules, $\mu := \frac{\sigma^E}{\sigma^I \lambda_m(\bar{\Lambda}^I)}$, where $\lambda_m(\cdot)$ denotes the smallest eigenvalue. Then, we introduce the second singular parameter $\varepsilon_I := \mu \varepsilon_E = \frac{1}{\sigma^I \lambda_m(\bar{\Lambda}^I)}$, so the system may be written as

$$\dot{x}_e = f_e(x_e, \eta, \xi) \quad (31a)$$

$$\varepsilon_E \dot{\eta} = -\bar{\Lambda}^E \eta + \varepsilon_E f_\eta(x_e, \eta, \xi) \quad (31b)$$

$$\varepsilon_I \dot{\xi} = -\frac{1}{\lambda_m(\bar{\Lambda}^I)} \bar{\Lambda}^I \xi + \varepsilon_I f_\xi(x_e, \eta, \xi), \quad (31c)$$

where f_η is defined in (28) and, after (23), (33), and (30),

$$f_\xi(x_e, \eta, \xi) = F_\xi \left([W \otimes I_n] \begin{bmatrix} x_e \\ \eta \end{bmatrix}, \xi \right) \quad (32)$$

The system (31) is in standard singular-perturbation form [24], albeit with three-time scales. As explained at the end of

Section II, there co-exist three dynamical systems: Eq. (31a), which is the slowest, corresponds to the weighted average of all nodes’ states; Eq. (31b), which is moderately fast, corresponds to the projection of the inter-modular synchronization errors e_η —see (26). Eq. (31c), which is the fastest, corresponds to a projection of the intra-modular synchronization errors e_k —see (11).

In the next section we present our main statement on stability for (7); we rely on the analysis of (31), via the following lemma that establishes asymptotic stability of the origin for (31), on arbitrary compacts of the state.

Lemma 2 (corollary of Theorem 11.3 in [24]): Consider the nonlinear autonomous singularly-perturbed system,

$$\dot{x} = f(x, z) \quad (33a)$$

$$\varepsilon \dot{z} = Az + \varepsilon g(x, z), \quad (33b)$$

where $x \in \mathbb{R}^{n_x}$, $z \in \mathbb{R}^{n_z}$ and $A \in \mathbb{R}^{n_z \times n_z}$ Hurwitz. Assume that the equilibrium $(x, z) = (0, 0)$ is an isolated equilibrium point and, for any $R > 0$, f and g are Lipschitz for all $(x, z) \in B_R$, with $B_R := \{(x, z) \in \mathbb{R}^{n_x \times n_z} : |x|^2 + |z|^2 < R^2\}$, with a Lipschitz constant $L(R)$. In addition, assume that for each $R > 0$ there exist positive definite decrescent functions V and $W : B_R \rightarrow \mathbb{R}_{\geq 0}$, positive constants $\alpha_1, \alpha_2, \beta$, as well as positive-definite functions $\phi_1 : B_R \rightarrow \mathbb{R}$ and $\phi_2 : B_R \rightarrow \mathbb{R}$, given by $\phi_1(x) = |x|$, $\phi_2(z) = |z|$, such that, for all $(x, z) \in B_R$,

$$\frac{\partial V}{\partial x} f(x, 0) \leq -\alpha_1 \phi_1(x)^2, \quad (34)$$

$$\frac{\partial W}{\partial z} Az \leq -\alpha_2 \phi_2(z)^2, \quad (35)$$

$$\frac{\partial V}{\partial x} [f(x, z) - f(x, 0)] \leq \beta \phi_1(x) \phi_2(z). \quad (36)$$

Let $L_1(R) > 0$ and $L_2(R) > 0$ be Lipschitz constants satisfying, for all $x \in B_R$ and $z \in B_R$,

$$|g(x, z) - g(0, z)| \leq L_1(R)|x|, \quad (37a)$$

$$|g(0, z)| \leq L_2(R)|z|. \quad (37b)$$

Then, for all $\varepsilon < \varepsilon^* := \frac{\alpha_1 \alpha_2}{\alpha_1 L_2(R) + \beta L_1(R)} > 0$, the origin of (33) is asymptotically stable and attractive to all trajectories that are contained in B_R . \square

Proof: Lemma 2 is a corollary of Theorem 11.3 in [24]. First, we recall that for the singularly-perturbed system (33), $h(x)$, the *quasi-steady-state*, is obtained by solving equation (33b) for $\varepsilon = 0$. Since A is Hurwitz by assumption, $h(x) = 0$.

Next, [24, Theorem 11.3] establishes the asymptotic stability of $(x, y) = (0, 0)$, where $y = z - h(x)$. Then, for $h(x) = 0$, the result is valid for $(x, z) = (0, 0)$ and [24, Theorem 11.3] can be used for the asymptotic stability of the origin (x, z) for the system (33).

Furthermore, notice that (11.39), (11.40) and (11.43) in [24] are equivalent to (34)–(36), for $h(x) = 0$ and $y = z$. Hence, [24, Eq. (11.44)] is satisfied since the boundary-layer system, $\frac{dz}{d\tau} = Az$ with $\tau = t/\varepsilon$ depends only on z and so does the function $W(z)$ associated with it. Finally, given the particular form of the system (33) and the satisfaction of (37) by assumption, we recover [24, Eq. (11.46)] with $\beta_2 = L_1(R)$ and $\gamma = L_2(R)$. \blacksquare

IV. NETWORK STABILITY ANALYSIS

Theorem 1: Consider the networked system (7) under Assumptions 1 and 2, and in its equivalent form (27)-(18b). Assume that for any $R > 0$, there exists a positive-definite decrescent, once continuously differentiable, function $V_e : \mathbb{R}^n \rightarrow \mathbb{R}_{\geq 0}$ and positive constants q_1 and c_1 , such that

$$\frac{\partial V_e}{\partial x_e} f_e(x_e, 0, 0) \leq -q_1 |x_e|^2 \quad (38)$$

$$\left| \frac{\partial V_e}{\partial x_e} \right| \leq c_1 |x_e|, \quad (39)$$

for all $x \in B_R$. Then, there exist $\sigma^{E^*} > 0$ and $\sigma^{I^*} > 0$ such that, for all $\sigma^I > \sigma^{I^*}$ and $\sigma^E > \sigma^{E^*}$, the origin for (7) is globally asymptotically stable. \square

Proof: By Lemma 1 the solutions of (1)-(2), equivalently those of (7), are globally bounded, that is, for any $r > 0$ there exist $R > 0$ such that

$$|x_o| \leq r \implies |x(t)| < R, \quad \forall t \geq 0. \quad (40)$$

In turn, in view of (13) and (25), $x_e(t)$, $\eta(t)$, $\xi(t)$ are also globally bounded. For simplicity, subject to a possible redefinition of R , we shall say that $|x_e(t)| < R$, $|\eta(t)| < R$, and $|\xi(t)| < R$ for all $t \geq 0$.

Then, the rest of the proof consists in applying Lemma 2 twice consecutively. One first time to show global asymptotic stability of the origin for the inter-modular dynamics on the synchronization manifold,

$$\dot{x}_e = f_e(x_e, \eta, 0) \quad (41a)$$

$$\dot{\eta} = -\sigma^E \bar{\Lambda}^E \eta + f_\eta(x_e, \eta, 0), \quad (41b)$$

where f_e and f_η are defined in (28) and (29) respectively, and a second time for the intra-modular dynamics

$$\dot{y} = f_y(y, \xi), \quad (42a)$$

$$\dot{\xi} = -\sigma^I \bar{\Lambda}^I \xi + g_\xi(y, \xi), \quad (42b)$$

where $y = [x_e^\top \ \eta^\top]^\top$,

$$g_\xi(y, \xi) = F_\xi([W^\dagger \otimes I_n]y, \xi),$$

$$f_y(y, \xi) := \begin{bmatrix} f_e(x_e, \eta, \xi) \\ -\sigma^E \bar{\Lambda}^E \eta + f_\eta(x_e, \eta, \xi) \end{bmatrix}.$$

1) Stability of the inter-modular dynamics: We analyze the system (41). To that end, we apply Lemma 2 with $x := x_e$, $z := \eta$, $\varepsilon := 1/\sigma^E$, $f(x, z) := f_e(x_e, \eta, 0)$, $g(x, z) := f_\eta(x_e, \eta, 0)$, and $A := -\bar{\Lambda}^E$. Next, consider (40). To verify (34) we pose $V(x) := V_e(x_e)$ so, after (38), (34) holds for all $x_e \in B_R$, with $\phi_1(x) := \sqrt{q_1} |x_e|$. Next, under Assumption 1, $-\bar{\Lambda}^E$ is Hurwitz, so there exists $P_\eta = P_\eta^\top > 0$, such that $\bar{\Lambda}^{E\top} P_\eta + P_\eta \bar{\Lambda}^E = 2I$. Therefore, (35) holds with $W(z) := \eta^\top P_\eta \eta$ and $\phi_2(z) := |\eta|$. Finally, condition (36) holds under Assumption 2 and after (39). Indeed, after (28) and (30)

$$f_e(x_e, \eta, 0) = [v_e^\top \otimes I_n] F_\zeta \left(\bar{P} [\mathbf{1}_m \otimes I_n] x_e + \bar{P} [W_1 \otimes I_n] \eta, 0 \right),$$

so invoking the Mean-value Theorem on each component of $F_\zeta(\cdot)$ above, we see that there exists $c(R)$ such that the left-hand side of (36) satisfies

$$\frac{\partial V_e}{\partial x_e} [f_e(x_e, \eta, 0) - f_e(x_e, 0, 0)] \leq c_1 c |x_e| |\eta| \quad (43)$$

for all $(x_e, \eta) \in B_R$. Therefore, (36) holds with $\beta := c_1 c$, $\alpha_1 = \sqrt{q_1}$ and $\alpha_2 = 1$. We conclude that for sufficiently large σ^{E^*} and any $\sigma^E \geq \sigma^{E^*}$, the origin $(x_e, \eta) = (0, 0)$ is asymptotically stable and all solutions that satisfy $x_e, \eta(t) \in B_R$ converge to zero. Furthermore, since $\sigma^{E^*} = \frac{1}{\varepsilon}$, $\sigma^{E^*} := \frac{\alpha_1 L_{\eta_2}(R) + \beta L_{\eta_1}(R)}{\alpha_1}$, given the continuous differentiability of f_η in B_R and the existence of $L_{\eta_1}(R)$ and $L_{\eta_2}(R)$ satisfying (37) for $g(x, z) = f_\eta(x_e, \eta, 0)$ with $f_\eta(0, 0, 0) = 0$. In other words, the origin is asymptotically stable for the inter-modular dynamics (the reduced-order network), and the origin is attractive on B_R , provided that the individual systems in each module M_k synchronize with their respective averages. This is established next.

2) Stability of the intra-modular dynamics: We turn now our attention to the overall system (27)-(42b), rewritten in the equivalent form (31), so we can apply Lemma 2; this time, with $x := [x_e^\top \ \eta^\top]^\top$, $z := \xi$, $g(x, z) := f_\xi(x_e, \eta, \xi)$ in (32), and

$$f(x, z) := \begin{bmatrix} f_e(x_e, \eta, \xi) \\ -\sigma^E \bar{\Lambda}^E \eta + f_\eta(x_e, \eta, \xi) \end{bmatrix}.$$

Let $V(x) := V_e(x_e) + \frac{1}{2} \eta^\top P_\eta \eta$, where P_η is defined in the previous paragraph and V_e is defined in the statement of the Theorem. Then, the left-hand side of Inequality (34) reads

$$\begin{aligned} \frac{\partial V}{\partial x} f(x, 0) &= \frac{\partial V_e}{\partial x_e} f_e(x_e, 0, 0) \\ &+ \frac{\partial V_e}{\partial x_e} [f_e(x_e, \eta, 0) - f_e(x_e, 0, 0)] \\ &- \frac{\sigma^E}{2} \eta^\top [\bar{\Lambda}^{E\top} P_\eta + P_\eta \bar{\Lambda}^E] \eta \\ &+ \eta^\top P_\eta f_\eta(0, \eta, 0) \\ &+ \eta^\top P_\eta [f_\eta(x_e, \eta, 0) - f_\eta(0, \eta, 0)]. \end{aligned} \quad (44)$$

The first term on the right-hand side of (44) satisfies (38) by assumption; the second term satisfies (43); the third is bounded by $-\sigma^E |\eta|^2$. Then, under Assumption 2, $f_\eta(0, \cdot, 0)$ is smooth and $f_\eta(0, 0, 0) = 0$, so by the Mean-value theorem (applied component-wise) it follows that for any $R > 0$ and all $\eta \in B_R$, $|f_\eta(0, \eta, 0)| \leq c_3(R) |\eta|$. After similar arguments and using (29) and (30), we conclude that the last term on the right-hand side of (44) satisfies

$$\eta^\top P_\eta [f_\eta(x_e, \eta, 0) - f_\eta(0, \eta, 0)] \leq c_4 |P_\eta| |x_e| |\eta| \quad (45)$$

for all $(x_e, \eta) \in B_R$. Thus, putting all these bounds together, we obtain

$$\begin{aligned} \frac{\partial V}{\partial x} f(x, 0) &\leq -q_1 |x_e|^2 + c_1 c |x_e| |\eta| - \sigma^E |\eta|^2 \\ &+ c_3 |P_\eta| |\eta|^2 + c_4 |P_\eta| |\eta| |x_e|, \end{aligned}$$

so there exists $\beta < 1$, such that (34) holds with $\phi_1(x) := \sqrt{\beta} \min\{q_1, \sigma^E\} |x_e^\top \ \eta^\top|^\top$ and $\alpha_1 = \sqrt{\beta} \min\{q_1, \sigma^E\}$.

The second inequality, (35), follows trivially with $W(z) := \frac{1}{2} \xi^\top P_\xi \xi$ where $P_\xi = P_\xi^\top$ solves the Lyapunov equation $\bar{\Lambda}^{I\top} P_\xi + P_\xi \bar{\Lambda}^I = 2I$, which holds since $-\bar{\Lambda}^I$ is Hurwitz. More precisely, since $\sigma^I = \frac{1}{\lambda_m(\bar{\Lambda}^I) \varepsilon_I}$ it follows that $\alpha_2 = \frac{1}{\lambda_m(\bar{\Lambda}^I)}$.

Finally, to see that Inequality (36) holds, we first observe that the left-hand side of (36) equals to

$$\frac{\partial V_e}{\partial x_e} [f_e(x_e, \eta, \xi) - f_e(x_e, \eta, 0)] + \eta^\top P_\eta [f_\eta(x_e, \eta, \xi) - f_\eta(x_e, \eta, 0)],$$

both of which, again by virtue of the differentiability of f_e and f_η , satisfy upper bounds that are linear in $|\xi|$ for all $x \in B_R$ and all $\xi \in B_R$. Thus, after (39), we have

$$\frac{\partial V}{\partial x} [f(x, z) - f(x, 0)] \leq c[c_1|x_e| + |P_\eta||\eta|]|\xi|,$$

so, since $\max\{|\eta|, |x_e|\} \leq |x|$, (36) follows with $\phi_1(x) := \alpha_1|x|$, $\phi_2(z) := |\xi|$, and $\beta := c \max\{c_1, |P_\eta|\}$.

Finally, given the continuous differentiability of f_ξ in B_R , there exist $L_{\xi 1}(R)$ and $L_{\xi 2}(R)$ such that $g(x, z) = f_\xi(x_e, \eta, \xi)$ with $f_\xi(0, 0, 0) = 0$ satisfies (37). Thus, we set $\sigma^{I*} := \frac{\alpha_1 L_{\xi 2}(R) + \beta L_{\xi 1}(R)}{\alpha_1 \alpha_2}$.

The statement of Theorem 1 follows. ■

V. APPLICATION TO NETWORK STABILIZATION

Theorem 1 guarantees global asymptotic stability of the origin, provided that Inequality (38) holds. In other words, if the origin for the average dynamics (31a) on the synchronization manifold $\{(\eta, \xi) = (0, 0)\}$,

$$\dot{x}_e = f_e(x_e, 0, 0), \quad (46)$$

is globally asymptotically stable. In this section we explore two control methods to stabilize the origin for (7) in the case that the average dynamics (46) is not GAS. The standing assumption is that each control $u_{k,i}$ in (5a) may be endowed with an additional input $v_{k,i}$. That is, we redefine

$$u_{k,i} = u_{k,i}^I + u_{k,i}^E + v_{k,i}, \quad (47)$$

so, in compact form, the network equation (7) becomes

$$\dot{x} = F(x) - \sigma^I [L^I \otimes I_n]x - \sigma^E [L^E \otimes I_n]x + v(x, x_c), \quad (48)$$

where the new input $v := [v_{1,1}^\top \cdots v_{1,N_1}^\top \cdots v_{m,1}^\top \cdots v_{m,N_m}^\top]$ depends on the network's state x and a distributed dynamics controller's state x_c to be defined.

We describe below two approaches that rely on modifying both the network's topology (and dimension) and the dynamics of (46) to render the origin GAS. We do this by adding control nodes to the network owing to two different strategies. The first consists in adding nodes to selected modules and the second consists in adding one or several whole control modules. The new nodes may be regarded as dynamic controllers that are added strategically using the coupling control inputs $v_{k,i}$.

These control approaches are explained in further detail below and illustrated in Figure 2.

A. Stabilization via control nodes added to modules

Let $k \leq M$ be arbitrarily fixed and let N'_k be a number of added nodes to the k th module. Then, the dynamics of each node originally present in the module, becomes

$$\dot{x}_{k,i} = f_{k,i}(x_{k,i}) + u_{k,i}^I + u_{k,i}^E + v_{k,i} \quad (49)$$

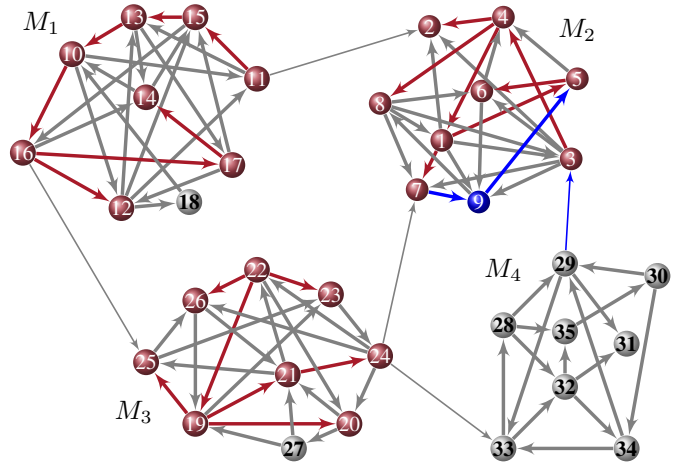


Fig. 2. Illustration of network control methods. Given a network of three modules M_1 , M_2 and M_3 containing eight nodes each, one control node is added to each module, as well as a whole control module, M_4 . Original nodes are in red, control modules are in gray and blue. Note that each module contains a directed spanning tree (emphasized in red). Also a spanning tree exists from modules M_1 to modules M_2 and M_3 . However, the overall network does not have a spanning tree without the added blue control node no. 9 in M_2 and the added blue links or the module M_4 .

$$v_{k,i} = -\sigma^I \sum_{j=1}^{N'_k} a'_{k,i,j} (x_{k,i} - x_{k,N_k+j}), \quad (50)$$

where

$$a'_{k,i,j} := \begin{cases} 1 & \text{if there is an edge from } (k,i) \text{ to } (k,j) \\ 0 & \text{otherwise;} \end{cases} \quad (51)$$

that is, $v_{k,i} \neq 0$ only for existing nodes interconnected to new nodes. Furthermore, by convention, the states of the N'_k added control nodes are labeled $x_{k,N_k+j} \in \mathbb{R}^n$ and their individual dynamics are given by

$$\dot{x}_{k,N_k+j} = f_{k,N_k+j}(x_{k,N_k+j}) - \sigma^I \sum_{i=1}^{N_k} a'_{k,j,i} (x_{k,N_k+j} - x_{k,i}). \quad (52)$$

Eq. (52) represents the dynamics of the control nodes, i.e., x_c in (48) is defined by all the applicable states x_{k,N_k+j} . As a result, the network (48) is transformed as follows. In compact form, the state vector, augmented by the states of the new nodes, corresponds to

$$\tilde{x} := [x_{1,1}^\top \cdots x_{1,N_1+1}^\top \cdots x_{1,N_1+N'_1}^\top \cdots x_{m,1}^\top \cdots x_{m,N_m+N'_m}^\top].$$

Then, proceeding as in Section II, akin to Eq. (7), we obtain the dynamics equation for the augmented network,

$$\dot{\tilde{x}} = \tilde{F}(\tilde{x}) - \sigma^I [\mathcal{L}^I \otimes I_n] \tilde{x} - \sigma^E [\mathcal{L}^E \otimes I_n] \tilde{x}, \quad (53)$$

where \tilde{F} corresponds to the function F in (6) augmented by the corresponding functions f_{k,N_k+j} in (52); while \mathcal{L}^I , $\mathcal{L}^E \in \mathbb{R}^{\mathcal{N} \times \mathcal{N}}$, with $\mathcal{N} := N + \sum_{k=1}^M N'_k$ are, respectively, the augmented internal and external Laplacians, as per the definition introduced in Section II. Thus, the augmented system (53) has the same structure as (7). In particular, the stability of the origin $\{\tilde{x} = 0\}$ depends on the dynamics of the added nodes (52) rendering the origin globally asymptotically stable

for the augmented average system, with $\{\xi = 0\}$ and $\{\eta = 0\}$. That is, for the system

$$\dot{x}_e = \sum_{k=1}^m \sum_{i=1}^{N_k+N'_k} w_{\ell k} v_{\ell k i} f_{k,i}(x_e), \quad (54)$$

where $w_{\ell}, v_{\ell k}$ are defined in the same way as in Section III for the new matrices $\mathcal{L}^I, \mathcal{L}^E$. We conclude this reasoning with the following statement, which stems directly from Theorem 1.

Corollary 1: Consider the networked system (48) under Assumptions 1 and 2, with modified individual dynamics as in (49)-(50) and the dynamic control extensions (52). Assume, in addition, that the origin for (54) is globally asymptotically stable and there exists a continuously differentiable Lyapunov function $V_e: \mathbb{R}^n \rightarrow \mathbb{R}_{\geq 0}$ satisfying (38)-(39), with $f_e(x_e, 0, 0)$ corresponding to the right-hand side of (54). Then, there exist $\sigma^{E^*} > 0$ and $\sigma^{I^*} > 0$ such that, for all $\sigma^I > \sigma^{I^*}$ and $\sigma^E > \sigma^{E^*}$, the origin for (53) system is GAS. \square

Illustrative example: Consider a network of $N = 24$ Lorenz oscillators with state $x_{k,i} := [x_{k,i} \ y_{k,i} \ z_{k,i}]^\top$ and dynamics

$$\dot{x}_{k,i} = H_{k,i}(x_{k,i})x_{k,i}, \quad H_{k,i} := \begin{bmatrix} -\sigma_{k,i} & \sigma_{k,i} & 0 \\ \rho_{k,i} & -1 & -x_{k,i} \\ 0 & x_{k,i} & -\beta_{k,i} \end{bmatrix}$$

where $\sigma_{k,i}, \beta_{k,i}, \rho_{k,i}$ are positive constants. Let these systems be interconnected over a strongly connected directed network that can be compartmentalized into $m = 3$ modules containing each $N_k = 8$ nodes. Let each module $k \in \{1, 2, 3\}$ constitute a strongly-connected sub-network with Laplacian

$$L_k^I = \begin{bmatrix} 4 & -1 & -1 & 0 & -1 & 0 & -1 & 0 \\ -1 & 4 & -1 & -1 & 0 & -1 & 0 & 0 \\ 0 & -1 & 4 & -1 & 0 & -1 & -1 & 0 \\ -1 & -1 & 0 & 5 & -1 & -1 & 0 & -1 \\ -1 & 0 & 0 & -1 & 3 & -1 & 0 & 0 \\ 0 & -1 & 0 & -1 & -1 & 5 & -1 & -1 \\ 0 & 0 & -1 & 0 & -1 & 0 & 3 & -1 \\ -1 & 0 & -1 & 0 & 0 & -1 & 0 & 3 \end{bmatrix}. \quad (55)$$

On the other hand, the elements of the external Laplacian $L^E \in \mathbb{R}^{24 \times 24}$ are set to $[L^E]_{1,1} = 2$, $[L^E]_{i,i} = 1$ for $i \in \{9, 17\}$, $[L^E]_{i,j} = -1$ for all $(i,j) \in \{(1,9), (1,17), (9,17), (17,1)\}$, and $[L^E]_{i,j} = 0$ otherwise. L^E contains mostly zero entries since the modules are sparsely connected. As matter of fact, the network may be represented as a strongly-connected network of modules, as shown in Figure 3.

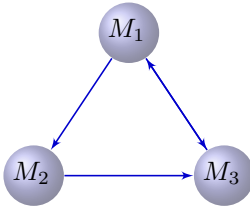


Fig. 3. Schematic representation of the inter-modular network

Then, the averaged dynamics x_e for this network yields

$$\dot{x}_e = \sum_{k=1}^m \sum_{i=1}^{N_k} w_{\ell k} v_{\ell k i} H_{k,i}(x_{e1})x_e. \quad (56)$$

For certain values of $\sigma_{k,i}, \beta_{k,i}, \rho_{k,i}$, set differently for all oscillators, the network reach consensus. That is, all oscillators converge to a stable equilibrium point, but different from the origin.

To enforce the global stabilization of the origin, to each module we add one node (*i.e.*, $N'_k = 1$) with dynamics $\dot{x}_{k,9} = [-\alpha x_{k,9} \ -\alpha y_{k,i} \ 0]^\top$ and we interconnect it to the first and third nodes. That is, in (49) we set

$$v_{k,i} = -\sigma^I(x_{k,i} - x_{k,9}) \quad \forall i \in \{1, 3\} \quad (57)$$

and $v_{k,i} = 0$ for all $i \in \{2, 4, 5, 6, 7, 8\}$. Then, we obtain the modified averaged dynamics, corresponding to the augmented network,

$$\dot{x}_e = \sum_{k=1}^m \sum_{i=1}^{N_k} w_{\ell k} v_{\ell k i} H_{k,i}(x_{e1})x_e + \sum_{k=1}^m \sum_{i=N_k+1}^{N_k+N'_k} w_{\ell k} v_{\ell k i} \begin{bmatrix} -\alpha \\ -\alpha \\ 0 \end{bmatrix} x_{e1} \quad (58)$$

which corresponds to Eq. (54).

Now, let

$$\sigma^* := \sum_{k=1}^m \sum_{i=1}^{N_k} w_{\ell k} v_{\ell k i} \sigma_{k,i}, \quad \rho^* := \sum_{k=1}^m \sum_{i=1}^{N_k} w_{\ell k} v_{\ell k i} \rho_{k,i}, \\ \omega_1^* := \sum_{k=1}^m \sum_{i=1}^{N_k} w_{\ell k} v_{\ell k i}, \quad \omega_2^* := \sum_{k=1}^m \sum_{i=N_k+1}^{N_k+N'_k} w_{\ell k} v_{\ell k i}$$

Then, using these definitions, (58) becomes

$$\dot{x}_e = \begin{bmatrix} -\sigma^* - \alpha \omega_2^* & \sigma^* & 0 \\ \rho^* & -\alpha \omega_2^* - \omega_1^* & -\omega_1^* x_{e1} \\ 0 & \omega_1^* x_{e1} & -\beta^* \end{bmatrix} x_e. \quad (59)$$

It is left to set α so that the origin for (59) be GAS. To that end, we remark that $\sigma^*, \rho^*, \omega_1^*$ and ω_2^* are all positive since, for this example, so are $w_{\ell k}$ and $v_{\ell k i}$. A straightforward computation, using the Lyapunov function $\mathcal{V}(x_e) = \frac{1}{2} \|x_e\|^2$, shows that $\dot{\mathcal{V}}(x_e) \leq -q \|x_e\|^2$, with $q > 0$, for any $\alpha > \max\{\frac{(\rho^* + \sigma^*)^2 - 2\sigma^*}{2\omega_2^*}, \frac{(\rho^* + \sigma^*)^2 - 2\omega_1^*}{2\omega_2^*}\}$.

In Figure 4 we show the result of a simulation of the augmented network as described above, with $\alpha = 30$. It is appreciated that the origin is asymptotically stable.

Figure 6 shows the trajectories of the systems in the network when Assumption 1 is not satisfied. In this case, the system's three time-scale behavior is reduced to a two time-scale behavior. In fact, we can see in the figure that the nodes of the network find general agreement whether they are of the same module or different modules. This is in contrast to Fig 5, in which we see that, initially, nodes of the same module find local agreement, leading to the formation of three clusters. In a second phase, the three trajectories merge, before stabilizing at the origin.

B. Stabilization via added control modules

We present now the second control approach to stabilize the origin for the network (7). It consists in adding new whole modules with the aim, as in the previous section, to render the

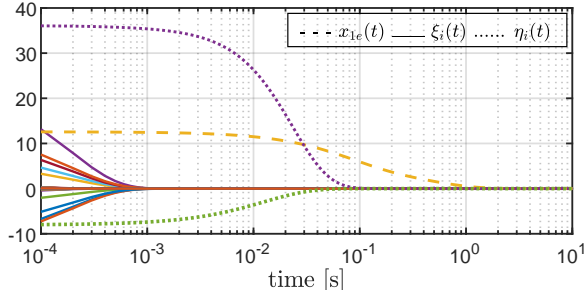


Fig. 4. Trajectories of the closed-loop system in logarithmic time scale. The solid lines represent the synchronization errors of the individual nodes relative to the modules' averages. The dotted lines represent the synchronization errors of each module relative to the modules' average. The dashed line depicts the overall average system's trajectories. In this simulation we used $\sigma^I = 5000$, $\sigma^E = 300$

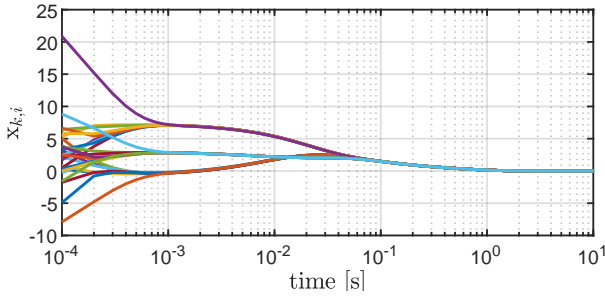


Fig. 5. Trajectories of the closed-loop system in logarithmic time scale, with $\sigma^I = 5000$, $\sigma^E = 300$

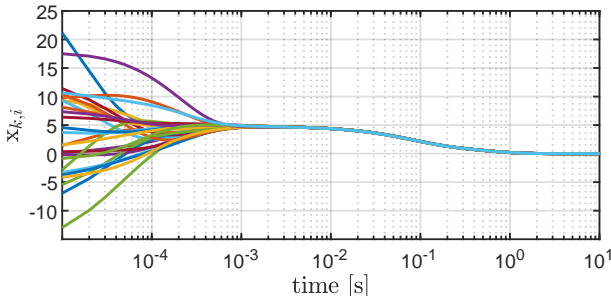


Fig. 6. Trajectories of the closed-loop system in logarithmic time scale, with $\sigma^I = 5000$, $\sigma^E = 12470 > \sigma^I \frac{|L^I|}{|L^E|}$

origin GAS for the resulting average system corresponding to the augmented network, on the synchronization manifold.

Let m' denote the number of new modules. For each $k' \leq m'$, the dynamics of the i th node within the k' th module is given by

$$\begin{aligned} \dot{x}_{m+k',i} = & f_{m+k',i}(x_{m+k',i}) \\ & - \sigma^I \sum_{l=1}^{N_{m+k'}} b_{m+k',i,l}(x_{m+k',i} - x_{m+k',l}) \\ & - \sigma^E \sum_{k=1}^m \sum_{j=1}^{N_k} a''_{(m+k',i),(k,j)}(x_{m+k',i} - x_{k,j}) \end{aligned} \quad (60)$$

where the coefficients $b_{m+k',i,l}$ represent internal interconnec-

tions within the $(m+k')$ th module, *i.e.*,

$$b_{m+k',i,l} := \begin{cases} 1 & \text{if there is an edge from } (m+k',i) \text{ to} \\ & (m+k',l) \\ 0 & \text{if otherwise.} \end{cases}$$

The coefficients $a''_{(m+k',i),(k,j)}$ represent external interconnections from nodes within the new control modules to nodes in the original network. That is,

$$a''_{(m+k',i),(k,j)} := \begin{cases} 1 & \text{if there is an edge from the node } (k,j) \\ & \text{to the node } (m+k',i) \\ 0 & \text{if otherwise.} \end{cases}$$

Correspondingly, the coupling

$$v_{k,i} = -\sigma^E \sum_{k'=1}^{m'} \sum_{j=1}^{N_{m+k'}} a''_{k,k',i,j}(x_{k,i} - x_{m+k',j}) \quad (61)$$

is added to the existing nodes in the original network. Note that only for those existing nodes that are interconnected to nodes within new modules $v_{k,i} \neq 0$.

The state of the resulting augmented network now is $\tilde{x} := [x_{1,1}^\top \cdots x_{1,N_1}^\top \cdots x_{m+1,1}^\top \cdots x_{m+m',N_{m+m'}}^\top]^\top$. That is, the augmented network in closed loop yields

$$\dot{\tilde{x}} = \tilde{F}(\tilde{x}) - \sigma^I [\mathcal{M}^I \otimes I_n] \tilde{x} - \sigma^E [\mathcal{M}^E \otimes I_n] \tilde{x}, \quad (62)$$

where \tilde{F} corresponds to the function F in (6) augmented by the corresponding functions $f_{m+k',i}$ in (60), \mathcal{M}^I and \mathcal{M}^E are, respectively, the new internal and external Laplacians, akin to L^I and L^E as per the definition of the latter below (7). Hence, since the closed-loop system (62) has the same structure as (7), the arguments in Section III apply. Notably, one can compute eigenvectors w_{lk} and v_{lki} as defined in (24) and (10) applying the appropriate transformations (as per in Section III) to \mathcal{M}^I and \mathcal{M}^E . Then, the new average dynamics, on the synchronization manifold, is

$$\dot{x}_e = \sum_{k=1}^{m+m'} \sum_{i=1}^{N_k} w_{lk} v_{lki} f_{k,i}(x_e). \quad (63)$$

From this reasoning we draw the following statement, which follows directly from Theorem 1.

Corollary 2: Consider the networked system (48) with modified dynamics as in (49), additional inputs (61) and the dynamic control extensions (60). Let Assumptions 1 and 2 hold for the resulting augmented closed-loop system (62) and assume, in addition, that the origin for the average system (63) is globally asymptotically stable and there exists a continuously differentiable Lyapunov function: $V_e : \mathbb{R}^n \rightarrow \mathbb{R}_{\geq 0}$ satisfying (38)-(39). Then, there exists $\sigma^{E*} > 0$ and $\sigma^{I*} > 0$ such that, for all $\sigma^I > \sigma^{I*}$ and $\sigma^E > \sigma^{E*}$, the origin of the closed-loop system (62) is GAS. \square

Illustrative example: To enforce the global stabilization with the second strategy, we add a control module to the original network. This 4th module contains $N_{4\top} = 8$ nodes with dynamics $\dot{x}_{4,i} = [-\alpha x_{4,i} \quad -\alpha y_{4,i} \quad 0]^\top$, furthermore, we consider that within this module, nodes are connected with respect to the Laplacian (55). A directed link is added from the first node of the control module to the first node of the other

modules $k \in \{1, 2, 3\}$ and a directed link from the first node of the third module to the first node of the control module. That is, in (49) we set

$$v_{k,1} = -\sigma^E(x_{k,1} - x_{9,1}) \quad \forall k \in \{1, 2, 3\}, \quad (64)$$

and $v_{k,i} = 0$ for all $i \in \{2, 3, 4, 5, 6, 7, 8\}$. Finally, in (60), only $a''_{(4,1),(3,1)} = 1$ and all other coefficients are set to zero. The value of the control parameter α may be computed as for the previous example. The systems' trajectories are showed in Figure 7 below.

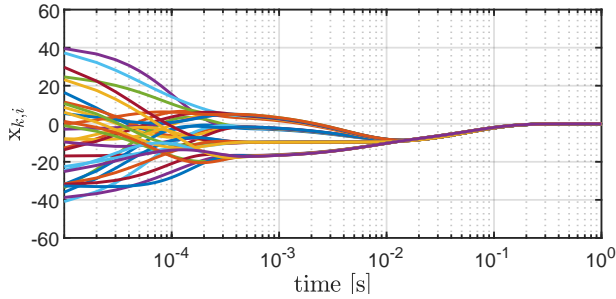


Fig. 7. Trajectories of the closed-loop system in logarithmic time scale, with $\sigma^I = 9000$, $\sigma^E = 900$

Thus, it may be appreciated from Figures 5 and 7 that, in spite of their simplicity, both control methods are efficacious to globally stabilize the origin for heterogeneous modular networks. In both figures the three-time scales behavior is well apparent. Indeed, in a first stage, the fastest trajectories $\xi(t)$ converge while $\eta(t)$ and $x_e(t)$ remain “constant” (on a logarithmic scale—see Figure 4). Then, as $\xi(t)$ approaches the origin, $\eta(t)$ converges as well, and $x_e(t)$ remains “constant”. Finally, $x_e(t)$ vanishes too, after $\eta(t)$ is close to zero.

VI. CONCLUSION

We provided a stability analysis of networked systems with modular structure. The setting is fairly general since we consider generic directed networks (containing a spanning tree, which is a necessary condition for consensus); it covers heterogeneous nonlinear systems; and the network's interconnections may have different weights. We showed that if there exist modules of densely interconnected nodes with strong interconnections, the network dynamics is captured by a model evolving in three time scales. Moreover, such modular structure is particularly useful to devise a control approach that consists in adding control nodes that modify the network's behavior at will.

Modular networks are common in varied engineering large-scale systems, such as power networks. This leads to the study of a whole range of new control problems for networked systems that deserve attention. In particular, the study of orbital stability for directed modular networks deserves attention since orbital stability is a pertinent property in the realm of nonlinear oscillators, as in the case of power generators.

REFERENCES

- [1] E. Panteley and A. Loría, “Synchronization and dynamic consensus of heterogeneous networked systems,” *IEEE Trans. on Automatic Control*, vol. 62, no. 8, pp. 3758–3773, 2017.
- [2] E. Steur, I. Tyukin, A. Gorban, N. Jarman, H. Nijmeijer, and C. Leeuwen, “Coupling-modulated multi-stability and coherent dynamics in directed networks of heterogeneous nonlinear oscillators with modular topology,” *IFAC-PapersOnLine*, vol. 49, pp. 62–67, 12 2016.
- [3] G. De Pasquale and M. E. Valcher, “Consensus for clusters of agents with cooperative and antagonistic relationships,” *Automatica*, vol. 135, p. 110002, 2022.
- [4] I.-C. Morărescu, S. Martin, A. Girard, and A. Muller-Gueudin, “Coordination in networks of linear impulsive agents,” *IEEE Transactions on Automatic Control*, vol. 61, no. 9, pp. 2402–2415, 2016.
- [5] E. Biyik and M. Arcak, “Area aggregation and time scale modeling for sparse nonlinear networks,” *Syst. & Contr. Lett.*, vol. 57, pp. 142–149, 02 2008.
- [6] D. Gfeller and P. D. L. Rios, “Spectral coarse graining and synchronization in oscillator networks,” *Phys. Rev. Lett.*, vol. 100, no. 17, 2008.
- [7] D. Romeres, F. Dörfler, and F. Bullo, “Novel results on slow coherency in consensus and power networks,” in *Europ. Contr. Conf.*, 2013, pp. 742–747.
- [8] S. Martin, I.-C. Morărescu, and D. Nešić, “Time scale modeling for consensus in sparse directed networks with time-varying topologies,” in *IEEE Conf. Dec. Contr.*, 2016, pp. 7–12.
- [9] I.-C. Morărescu and R. Postoyan, “Dimension reduction for large-scale networked systems,” in *IEEE Conf. Dec. Contr.*, Maui, Hawaii, United States, Dec. 2012, pp. 4302–4307.
- [10] V. Varma, I.-C. Morărescu, and Y. Hayel, “Analysis and control of multi-levelled opinions spreading in social networks,” in *American Control Conference, ACC 2018*, Milwaukee, WI, United States, Jun. 2018.
- [11] M. Maghenem, E. Panteley, and A. Loría, “Singular-perturbations-based analysis of synchronization in heterogeneous networks: a case-study,” in *Proc. 55th IEEE Conf. Decision and Control*, Las Vegas, NV, USA, 2016, pp. 2581–2586.
- [12] B. Adhikari, I.-C. Morărescu, and E. Panteley, “An emerging dynamics approach for synchronization of linear heterogeneous agents interconnected over switching topologies,” *IEEE Control Systems Letters*, vol. 5, no. 1, pp. 43–48, 2021.
- [13] J. Chow and P. Kokotović, “Time scale modeling of sparse dynamic networks,” *IEEE Transactions on Automatic Control*, vol. 30, no. 8, pp. 714–722, 1985.
- [14] B. Adhikari, E. Panteley, and I.-C. Morărescu, “Three time scales modeling of the undirected clustered network,” in *2022 IEEE 61st Conference on Decision and Control (CDC)*, 2022, pp. 987–992.
- [15] A. Pogromsky, “Synchronization and adaptive synchronization in semi-passive systems,” in *Proc. 1st Int. Conf. Control of Oscillations and Chaos*, vol. 1, 1997, pp. 64–68 vol.1.
- [16] W. Yu, G. Chen, J. Lü, and J. Kurths, “Synchronization via pinning control on general complex networks,” *SIAM Journal on Control and Optimization*, vol. 51, no. 2, pp. 1395–1416, 2013.
- [17] A. Lazri, E. Panteley, and A. Loría, “On the robustness of networks of heterogeneous semi-passive systems interconnected over directed graphs,” e-print no. arXiv:2307.14868, July 2023, Available from <http://arxiv.org/abs/2307.14868>.
- [18] S. Monaco and L. R. Celsi, “On multi-consensus and almost equitable graph partitions,” *Automatica*, vol. 103, pp. 53–61, 2019.
- [19] M. Maghenem, E. Panteley, and A. Loría, “Singular-perturbations-based analysis of dynamic consensus in directed networks of heterogeneous nonlinear systems,” e-print no. arXiv:2205.15646, May 2022.
- [20] N. Monshizadeh, H. L. Trentelman, and M. K. Camlibel, “Projection-based model reduction of multi-agent systems using graph partitions,” *IEEE Transactions on Control of Network Systems*, vol. 1, no. 2, pp. 145–154, 2014.
- [21] L. Yu, X. Cheng, J. M. Scherpen, and J. Xiong, “Synchronization preserving model reduction of multi-agent network systems by eigenvalue assignments,” in *2019 IEEE 58th Conference on Decision and Control (CDC)*, 2019, pp. 7794–7799.
- [22] B. Besselink, H. Sandberg, and K. H. Johansson, “Clustering-based model reduction of networked passive systems,” *IEEE Transactions on Automatic Control*, vol. 61, no. 10, pp. 2958–2973, 2016.
- [23] X. Cheng, J. M. Scherpen, and B. Besselink, “Balanced truncation of networked linear passive systems,” *Automatica*, vol. 104, pp. 17–25, 2019.
- [24] H. K. Khalil, *Nonlinear systems; 3rd ed.* Upper Saddle River, NJ: Prentice-Hall, 2002.